

Dan Wei and Mary R. Loeken



Increased DNA Methyltransferase 3b (Dnmt3b)-Mediated CpG Island Methylation Stimulated by Oxidative Stress Inhibits Expression of a Gene Required for Neural Tube and Neural Crest Development in Diabetic Pregnancy



Diabetes 2014;63:3512–3522 | DOI: 10.2337/db14-0231

Previous studies have shown that diabetic embryopathy results from impaired expression of genes that are required for formation of embryonic structures. We have focused on *Pax3*, a gene that is expressed in embryonic neuroepithelium and is required for neural tube closure. *Pax3* expression is inhibited in embryos of diabetic mice due to hyperglycemia-induced oxidative stress. DNA methylation silences developmentally expressed genes before differentiation. We hypothesized that hypomethylation of *Pax3* upon neuroepithelial differentiation may be inhibited by hyperglycemia-induced oxidative stress. We tested this using embryos of pregnant hyperglycemic mice and mouse embryonic stem cells (ESC). Methylation of a *Pax3* CpG island decreased upon neurulation of embryos and formation of neuronal precursors from ESC. In ESC, this was inhibited by oxidative stress. Use of short hairpin RNA in ESC demonstrated that DNA methyltransferase 3b (Dnmt3b) was responsible for methylation and silencing of *Pax3* before differentiation and by oxidative stress. Although expression of *Dnmt3b* was not affected by oxidative stress, DNA methyltransferase activity was increased. These results indicate that hyperglycemia-induced oxidative stress stimulates Dnmt3b

activity, thereby inhibiting chromatin modifications necessary for induction of *Pax3* expression during neurulation and thus providing a molecular mechanism for defects caused by *Pax3* insufficiency in diabetic pregnancy.

Maternal pregestational diabetes significantly increases the risk for congenital malformations (1–6). Although many organ systems can be affected, neural tube defects (NTD) and cardiac outflow tract defects (COTD) are among the most common that occur (2,7). The malformations arise early during embryonic development, mostly within the first 8 gestational weeks, when organ systems are first starting to form (8). Results of human and animal studies indicate that hyperglycemic excursions during organogenesis are responsible for malformations induced by diabetic pregnancy (9).

Work from our laboratory has demonstrated that maternal hyperglycemia inhibits expression of *Pax3*, a gene that is expressed in embryonic neuroepithelium and neural crest and is required for neural tube and cardiac outflow tract formation (10–12). That homozygous

Section on Islet Cell and Regenerative Biology, Joslin Diabetes Center, and Department of Medicine, Harvard Medical School, Boston, MA

Corresponding author: Mary R. Loeken, mary.loeken@joslin.harvard.edu.

Received 10 February 2014 and accepted 10 May 2014.

This article contains Supplementary Data online at <http://diabetes.diabetesjournals.org/lookup/suppl/doi:10.2337/db14-0231/-DC1>.

The content of this article is solely the responsibility of M.R.L. and does not necessarily represent the official views of the National Institutes of Health.

© 2014 by the American Diabetes Association. Readers may use this article as long as the work is properly cited, the use is educational and not for profit, and the work is not altered.

mutant *Pax3* mouse embryos develop NTD and COTD with 100% penetrance (13,14) supports the notion that inhibition of *Pax3* below a critical threshold is sufficient to cause NTD or COTD in embryos of diabetic mothers. Several studies have indicated that oxidative stress produced in the embryo in response to increased glucose metabolism is responsible for diabetic pregnancy-induced malformations (15–20). We have shown that oxidative stress inhibits expression of *Pax3* (21,22). The precise mechanisms by which oxidative stress inhibits *Pax3* are not known.

During mammalian embryogenesis, methylation of DNA at cytosines is a dynamic process that serves several purposes, including gene silencing, chromosomal stability, and setting up parental gene imprinting patterns (23). In the inner cell mass (ICM) of the early embryo or in undifferentiated (UD) embryonic stem cells (ESC), genes that will be expressed in a lineage-dependent fashion upon differentiation are silenced by methylation at CpG dinucleotides (24–28). Upon tissue differentiation, induced expression of these genes requires epigenetic modifications, including hypomethylation of CpG dinucleotides (24–28). Dense clusters of CpG sequences, called CpG islands, are often located at mammalian gene promoters. Although CpG islands differ from most chromosomal DNA by infrequent cytosine methylation, many CpG islands located around genes that are expressed in a tissue-specific fashion and that are essential regulators of embryonic development (including members of the *Pax* gene family) display tissue-specific methylation (29).

Three known enzymes regulate DNA methylation, Dnmt1, Dnmt3a, and Dnmt3b. Dnmt1 maintains DNA methylation of daughter strands during replication, and Dnmt3a and Dnmt3b regulate de novo DNA methylation, for example, during differentiation (26,30).

Here we tested the hypothesis that *Pax3* expression is silenced before its onset of expression during neurulation by methylation of a CpG island within its transcriptional regulatory element and that oxidative stress, consequent to maternal hyperglycemia, preserves the hypermethylated state of this CpG island. Further, we tested the hypothesis that expression or activity of a DNA methyltransferase would be responsible for preservation of the hypermethylated state of the *Pax3*-associated CpG island.

RESEARCH DESIGN AND METHODS

Animal Procedures

All procedures using animals were approved by the Joslin Diabetes Center Institutional Animal Care and Use Committee. Nondiabetic female ICR mice were housed with nondiabetic ICR males and were checked daily for copulation plugs. Noon on the day that a copulation plug was found was determined to be embryonic day 0.5 (E 0.5). Transient hyperglycemia was induced in pregnant mice on E 7.5 by injecting 2 mL 12.5% glucose dissolved in PBS at approximately hourly intervals to maintain maternal blood glucose ≥ 16.65 mmol/L, as previously

described (12). Oxidative stress was induced on E 7.5 using 3 mg/kg antimycin A (AA; Sigma-Aldrich, St. Louis, MO), a dose that replicates the effects of maternal hyperglycemia to induce oxidative stress and inhibit *Pax3* expression, as previously described (12,21,22). Preimplantation embryos were flushed from uteri to recover blastocysts on E 3.5, and postimplantation embryos were dissected from uteri on E 8.5.

Culture of Murine ESC

Murine ESC of the D3 line were cultured and induced to differentiate into neuronal precursors, as previously described (31). Briefly, ESC were grown as UD monolayer cultures in DMEM (Life Technologies, Grand Island, NY) containing leukocyte inhibitory factor (Millipore, Billerica, MA) for 4 days, then differentiation was induced by forming embryoid bodies in nonadherent culture dishes in media without leukocyte inhibitory factor but containing 0.5 $\mu\text{mol/L}$ retinoic acid (Sigma-Aldrich) for 4 days. Embryoid bodies were placed into adherent culture dishes with the same media as used when forming embryoid bodies for 1 day, then the media were replaced with DMEM/F-12 (Life Technologies) containing fibronectin (Becton Dickinson), insulin, transferrin, and selenium (all from Sigma-Aldrich) for 4 additional days to select for differentiating neuronal precursors.

Oxidative stress was induced by adding 10 $\mu\text{mol/L}$ AA to the media used during selection of neuronal precursors, as described (31). This concentration of AA has been shown to significantly increase markers of oxidative stress and to inhibit *Pax3* expression by D3 ESC (31,32). A total of 10 $\mu\text{mol/L}$ of the DNA methyltransferase inhibitor, 5-azacytidine (AzaC, Sigma-Aldrich), was added to the media while culturing UD ESC or while selection for neuronal precursors.

RT-PCR Assays

E 3.5 blastocysts were recovered from 18 pregnant mice, and three to four blastocysts from six litters were pooled for three separate RT-PCR assays. E 8.5 embryos were recovered from three separate litters per treatment group, and embryos from each litter were pooled for RT-PCR assay. Four 60-mm culture dishes of UD ESC or ESC-derived neuronal precursors for each treatment group were used for separate RT-PCR assays. Total RNA was extracted from embryos or cells using Ultraspec reagent (Bioteex Laboratories, Friendswood, TX). The High-Capacity cDNA Reverse Transcription Kit from Life Technologies (Foster City, CA) was used to reverse transcribe 200 ng RNA. Real-time PCR was performed using TaqMan PCR Master Mix (Life Technologies) and primers, and a VIC-labeled probe was used to detect rRNA (Life Technologies #43189E) as the normalization control, as described (21). Primers and FAM-labeled probe for *Pax3* cDNA were as previously published (21). Primers and FAM-labeled probes for *p53* (Mm01731290_g1), *Pax6* (Mm00443081_m1), *Pax7* (Mm01354484_m1), *Dnmt1* (Mm01151063_m1), *Dnmt3a* (Mm00432881_m1), and

Dnmt3b (Mm01240113_m1) cDNA were obtained from Life Technologies.

5-Methylcytosine Immunoprecipitation Assays

E 3.5 blastocysts were recovered from 18 pregnant mice, and six to nine blastocysts from six litters were pooled for three separate 5-methylcytosine immunoprecipitation–DNA immunoprecipitation (mDIP) assays. E 8.5 embryos were recovered from three separate litters per treatment group, and embryos from each litter were pooled for mDIP assay. Three 60-mm culture dishes of UD ESC or ESC-derived neuronal precursors for each treatment group were pooled for mDIP assays. Genomic DNA was extracted, and mDIP assays were performed as described (33). Briefly, genomic DNA was sonicated using four cycles of 70% duty, 20% output, 10 pulses/cycle on ice to generate fragments of ~300–1,000 bp in length. Sonicated DNA (4 µg) was immunoprecipitated using 10 µL 5-methylcytosine antibody (Active Motif, Carlsbad, CA). After Proteinase K (Life Technologies) treatment, phenol chloroform extraction, and ethanol precipitation, the immunoprecipitated DNA was resuspended in 30 µL Tris-EDTA buffer. Immunoprecipitated DNA (1 µL) was amplified by PCR using SYBR green detection (Life Technologies), in quadruplicate, in a 10 µL final volume. Unimmunoprecipitated DNA (20 ng; input) were amplified in parallel as the normalization control. The primers used for amplification of the promoter-proximal *Pax3* and *p53* CpG islands and PCR conditions are listed in Supplementary Table 1. *Pax3* and *p53* CpG islands were chosen using the Genome Browser on the University of California Santa Cruz Bioinformatics site (<http://genome.ucsc.edu>). PCR primers were designed using the National Center for Biotechnology Information Primer-BLAST tool (http://www.ncbi.nlm.nih.gov/tools/primer-blast/index.cgi?LINK_LOC=BlastDescAd).

Bisulfite DNA Modification

Genomic DNA was prepared from cells pooled from three 60-mm culture dishes and was modified with sodium bisulfite using the BisulFlash DNA Modification Kit (Epigentek Group Inc., Brooklyn, NY), according to the manufacturer's instructions. The bisulfite-altered DNA was amplified to generate three overlapping PCR products within the *Pax3* CpG island using primers not containing CpG dinucleotides. PCR primer sequences are listed in Supplementary Table 2. All PCR reactions were performed using 40 cycles of denaturation at 95°C for 10 s, annealing at 55°C for 10 s, and extension at 72°C for 8 s. The PCR products were inserted into a TA cloning vector (Life Technologies) and used to transform competent DH5- α *Escherichia coli* (Life Technologies). DNA from 10 colonies containing each of the PCR inserts was sequenced, and contiguous sequences were analyzed for retention of cytosines or conversion to thymines. CpG methylation was analyzed using Quantification Tool for Methylation Analysis (QUMA) (<http://quma.cdb.riken.jp>, Kyoto, Japan) (34).

Inhibition of DNA Methyltransferase mRNA

Short hairpin RNA (shRNA) sequences targeting *Dnmt1*, *Dnmt3a*, or *Dnmt3b* mRNA were designed using the shRNA Sequence Designer (www.clontech.com). Three shRNA sequences targeted against each of the DNA methyltransferase RNA sequences (Supplementary Table 3) were inserted into the XhoI and *Hind*III sites of pSingle-TS-shRNA (Clontech, Mountain View, CA). Presence of inserts was determined by restriction digestion with *Mlu*I (Promega, Madison, WI). Transfection, selection of stably transformed cells, and induction of shRNA expression with doxycycline (Dox; Clontech) was as described (35). A scrambled sequence inserted into pSingle (35) was used as a control.

DNA Methyltransferase Activity Assay

Nuclear extracts were prepared from cells grown on 60-mm culture dishes in triplicate using an EpiQuik Nuclear Extraction Kit (Epigentek Group Inc.). DNA methyltransferase enzyme activity was assayed using a colorimetric EpiQuik DNMT Activity/Inhibition Assay Kit (Epigentek Group Inc.), according to the manufacturer's instructions. Activity was expressed relative to nuclear extract protein that was measured using Bio-Rad Protein Dye Reagent (Bio-Rad, Hercules, CA).

Statistical Analyses

Data were analyzed by one-way ANOVA, followed by the Tukey post hoc test or two-way ANOVA, followed by Bonferroni post test, using GraphPad Prism v. 4.0 software (La Jolla, CA). Specific tests used and comparisons made are indicated in the figure legends. $P < 0.05$ was determined to be statistically significant.

RESULTS

Association of *Pax3* CpG Island Methylation With *Pax3* Silencing in Embryos and ESC

We previously examined *Pax3* expression by embryos on E 8.5, when *Pax3* expression begins and the neural tube starts to form, from control pregnancies and from diabetic, transiently hyperglycemic, and oxidative stress-induced pregnancies (10,12,21). We hypothesized that cytosines within *Pax3* regulatory elements were hypermethylated before the onset of *Pax3* expression during embryogenesis and that hyperglycemia-induced oxidative stress blocked differentiation-associated *Pax3* hypomethylation. To test these hypotheses, we obtained embryos before the onset of *Pax3* expression (E 3.5 blastocysts) and on E 8.5. The E 8.5 embryos were obtained from pregnant mice that had been injected with glucose to induce transient hyperglycemia or with AA to induce oxidative stress, on E 7.5, or from uninjected controls. We previously showed that oxidative stress induced by maternal diabetes on E 7.5 prevents normal *Pax3* expression and leads to NTD (12,21).

To determine whether *Pax3* is selectively regulated by hyperglycemia and oxidative stress, we assayed expression of two additional *Pax* genes and *p53*. *Pax7* is a paralog of

Pax3, whose spatial pattern overlaps that of *Pax3* and whose expression begins slightly later than *Pax3* (36). Unlike *Pax3*, *Pax7* does not contain a promoter-proximal CpG island, according to the Genome Browser on the University of California Santa Cruz Bioinformatics site. *Pax6* is expressed in the ventral neural tube. Its dorsoventral expression restriction is inversely regulated to that of *Pax3* by signals emanating from the notochord (36,37). *p53*, like *Pax3*, contains a promoter-proximal CpG island, but unlike *Pax3*, *p53* is regulated posttranslationally, but not transcriptionally, by oxidative stress (38). Also, unlike *Pax3*, *p53* mRNA does not change upon differentiation of ESC to neuroepithelial-like neuronal precursors (35). As expected, *Pax3* expression significantly increased in E 8.5 embryos compared with E 3.5 blastocysts, and induction of hyperglycemia or oxidative stress on E 7.5 significantly inhibited *Pax3* expression on E 8.5 (Fig. 1A). However, although expression of *Pax7* and *Pax6* significantly increased between E 3.5 and E 8.5, there was no effect of hyperglycemia or oxidative stress on *Pax7* or *Pax6* expression. *p53* expression did not change between E 3.5 and 8.5 and was not inhibited by hyperglycemia or oxidative stress.

A 656-bp CpG island containing 49 CpG dinucleotides was identified near the *Pax3* start site of transcription (−169 to 487), as described in RESEARCH DESIGN AND METHODS. This sequence overlaps an element (−1,578 to 70) that is sufficient for a transgenic reporter plasmid expression in E 8.5 neuroepithelium (39). A 966-bp CpG island located upstream of and overlapping the transcriptions start site of the human *PAX3* gene has 79% identity with the 656-bp mouse element, suggesting a conserved regulatory function. Two smaller CpG islands are located ~6.7 kb 5' of the *Pax3* coding sequence and within an intron ~7.3 kb 3' of the start site of transcription; however, because neither element was contained within the transgene that directed neuroepithelial expression (39), we focused on the 656-bp CpG island. A 329-bp CpG island with 29 CpG dinucleotides is located near the *p53* promoter. Because *p53* mRNA expression was not regulated developmentally or by hyperglycemia or metabolism, the *p53* CpG island was used as a control during initial studies of the *Pax3* CpG island.

5-Methylcytosine genomic DNA from whole embryos was immunoprecipitated (mDIP) and then amplified by PCR with primers specific to the *Pax3* or *p53* CpG islands,

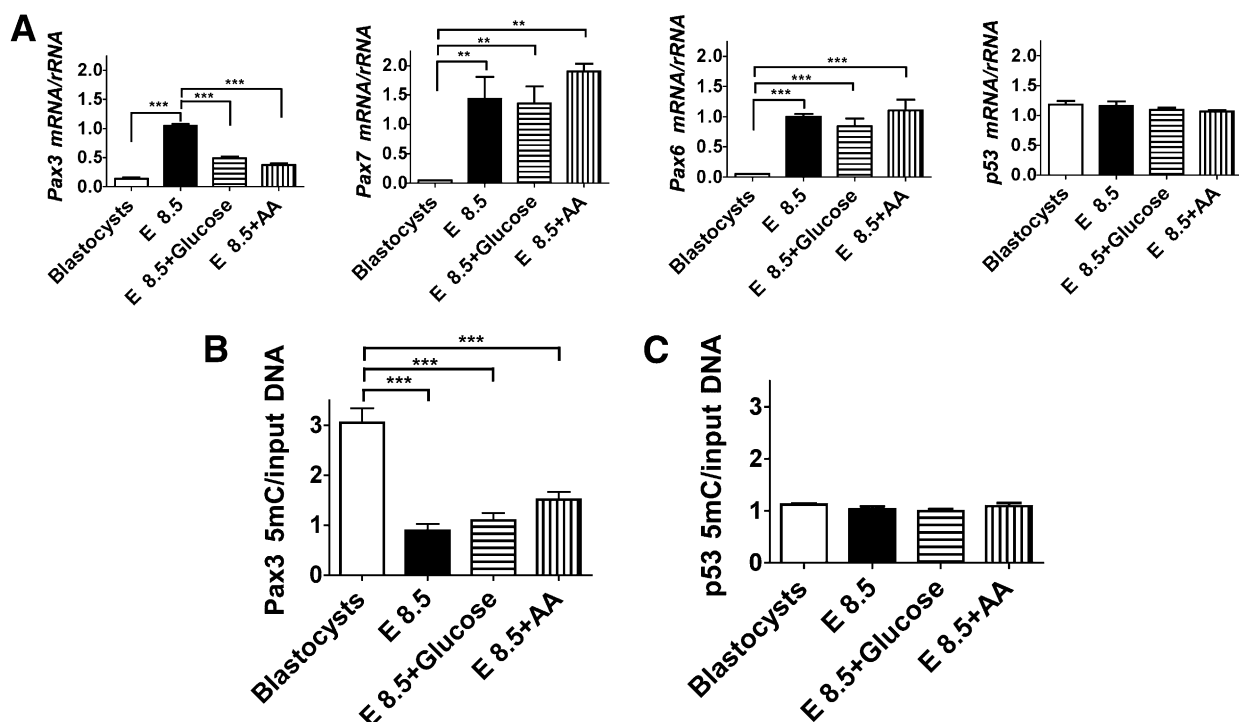


Figure 1—Embryo gene expression and CpG island methylation during differentiation from blastocysts to neurulating embryos and in response to maternal hyperglycemia or oxidative stress. *A*: RT-PCR of *Pax3*, *Pax7*, *Pax6*, or *p53* mRNA normalized to rRNA from E 3.5 blastocysts or E 8.5 embryos. E 8.5 embryos were obtained from control pregnant mice or mice in which transient hyperglycemia had been induced on E 7.5 with glucose or in which oxidative stress had been induced with AA. mRNA was expressed relative to gene expression in control E 8.5 embryos. *B*: mDIP assay of the *Pax3* CpG island from E 3.5 blastocysts or E 8.5 embryos from pregnancies treated as in *A*. *C*: mDIP assay of the *p53* CpG island from E 3.5 blastocysts or E 8.5 embryos from pregnancies treated as in *A*. *B* and *C*: Immunoprecipitated DNA was normalized to total DNA before immunoprecipitation (input) and expressed relative to immunoprecipitated DNA from E 8.5 embryos ($n = 3$ pools of blastocysts from 18 separate pregnancies or pooled embryos from 3 separate E 8.5 pregnancies). The error bars indicate the standard error. Data were analyzed by one-way ANOVA, followed by the Tukey post test. ** $P < 0.01$; *** $P < 0.001$.

as described in RESEARCH DESIGN AND METHODS. Significantly more of the *Pax3* CpG island was immunoprecipitated from blastocyst DNA than from E 8.5 embryos (Fig. 1B), consistent with the hypothesis that hypomethylation of this CpG island is involved in induction of *Pax3* expression. However, *Pax3* CpG island methylation in embryos from hyperglycemic or oxidative stress-induced pregnancies did not differ significantly compared with control E 8.5 embryos. Consistent with the constant *p53* mRNA expression in embryos of different developmental stages and regardless of exposure to oxidative stress, there was no difference in immunoprecipitated methylcytosine associated with the *p53* CpG island from any of the embryos (Fig. 1C).

It is possible that no difference in *Pax3* CpG island methylation was detected in E 8.5 embryos from hyperglycemic or oxidative stress-treated pregnancies, compared with control E 8.5 embryos, despite the significant inhibition of *Pax3* expression, because *Pax3* expression initiates on E 8.5, first in neuroepithelium and slightly later in somites (40), but *Pax3* expression in somites does not appear to be inhibited by maternal diabetes or oxidative

stress (10,11). Thus, lack of effect of oxidative stress on methylation of the *Pax3* CpG island in somites may obscure effects on the *Pax3* CpG island in neuroepithelium. We then turned to murine ESC as a cell culture model that is more homogenous than the whole embryo. We previously showed that *Pax3* is expressed upon induction of differentiation of neuronal precursors (resembling neuroepithelium) from UD monolayer cultures (derived from the blastocyst ICM), and that *Pax3* expression in ESC-derived neuronal precursors is inhibited by AA-induced oxidative stress (31,35).

mRNA and DNA were obtained from UD or differentiating (D) ESC, or from D ESC in which oxidative stress had been induced with AA during differentiation. AzaC, a DNA methyltransferase inhibitor, was added to UD and D cultures as a control. There was a slight but significant increase in *Pax3* expression in UD ESC treated with AzaC (Fig. 2A), suggesting that silencing of *Pax3* before its induction is partly due to DNA methylation. There was a significant increase in *Pax3* expression in D ESC, which was further increased by AzaC. AA significantly inhibited the increase in *Pax3* expression in D ESC. *Pax3* CpG island

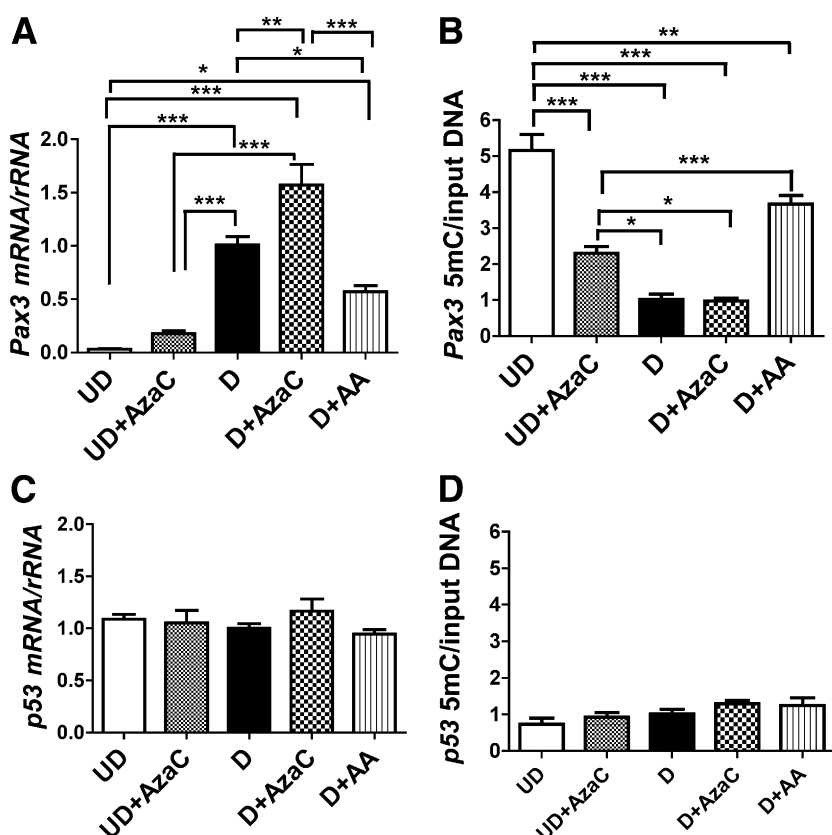


Figure 2—Gene expression and CpG island methylation during differentiation of ESC to neuronal precursors and during oxidative stress. *A*: RT-PCR of *Pax3* mRNA normalized to *rRNA* from UD ESC or ESC induced to differentiate into neuronal precursors (D), treated or not with AzaC or AA. *B*: mDIP assay of the *Pax3* CpG island from cultures treated as in *A*. *C*: RT-PCR of *p53* mRNA normalized to *rRNA* from the same cultures as in *A*. *D*: mDIP assay of the *p53* CpG island from the same cultures as in *B*. (For *A* and *C*, $n = 4$ culture dishes. For *B* and *D*, $n = 3$ culture dishes pooled and assayed in quadruplicate.) The error bars indicate the standard error. Data were analyzed by one-way ANOVA, followed by the Tukey post test. * $P < 0.05$; ** $P < 0.01$; *** $P < 0.001$.

methylation was inversely related to *Pax3* expression in UD, UD + AzaC, and D ESC (Fig. 2B), suggesting that, as in embryos, induction of *Pax3* expression is associated with hypomethylation of the *Pax3* CpG island. There was no further decrease in methylation of the *Pax3* CpG island in D ESC treated with AzaC, suggesting that the increase in *Pax3* expression in D ESC treated with AzaC was due to inhibition of methylation of other genes whose expression contributes to *Pax3* regulation. Notably, consistent with the hypothesis, methylation of the *Pax3* CpG island was significantly increased in D ESC treated with AA compared with control D ESC. There was no significant effect of differentiation, AzaC, or AA on *p53* mRNA levels or methylation of the *p53* CpG island (Fig. 2C and D), suggesting that expression of *p53* is not regulated by DNA methylation under these conditions.

To study localization as well as frequency of *Pax3* CpG island methylation, genomic DNA from UD, D, or D ESC treated with AA was treated with sodium bisulfite. Bisulfite deaminates cytosine, converting it to uracil, but 5-methylcytosine is resistant to this reaction (41). Thus, after PCR amplification of bisulfite-modified DNA, substitutions of cytosines with thymines is indicative of unmethylated cytosines, and retention of cytosines is indicative of 5-methylcytosines. After bisulfite modification, the *Pax3* CpG island (between -194 and 510) was amplified by PCR, as described in RESEARCH DESIGN AND METHODS. Ten colonies containing plasmids with CpG island fragments

from each treatment group were sequenced, and the sequences from the modified DNA were compared with the genomic sequence using QUMA (34) (Fig. 3A). The percent conversion of CpG dinucleotides of the sequenced CpG island fragments was 97–100%, as determined by QUMA. Notably, the mean percentage of methylated CpG dinucleotides significantly decreased between UD and D ESC (Fig. 3B). The locations of methylated CpG dinucleotides in D ESC treated with AA were similar to those in UD ESC, and the mean percentage of methylated CpG dinucleotides in D ESC treated with AA was significantly greater than in D ESC (Fig. 3A and B).

Dnmt3b Regulation of *Pax3* Expression and CpG Island Methylation During Differentiation and Oxidative Stress

To determine which Dnmt(s) regulated *Pax3* expression and CpG island methylation, we constructed Dox-inducible shRNA plasmids containing three different shRNA sequences that targeted each of the Dnmt transcripts. ESC were stably transformed with empty plasmid, plasmid containing a scrambled sequence, or one of the plasmids containing a Dnmt shRNA sequence. As shown in Fig. 4A–C, abundance of each of the Dnmt transcripts was knocked down both in UD and in D ESC upon treatment of cells with Dox but only in the cells transfected with specific shRNA sequences. Induction of each shRNA also decreased steady-state levels of each Dnmt protein (Supplementary

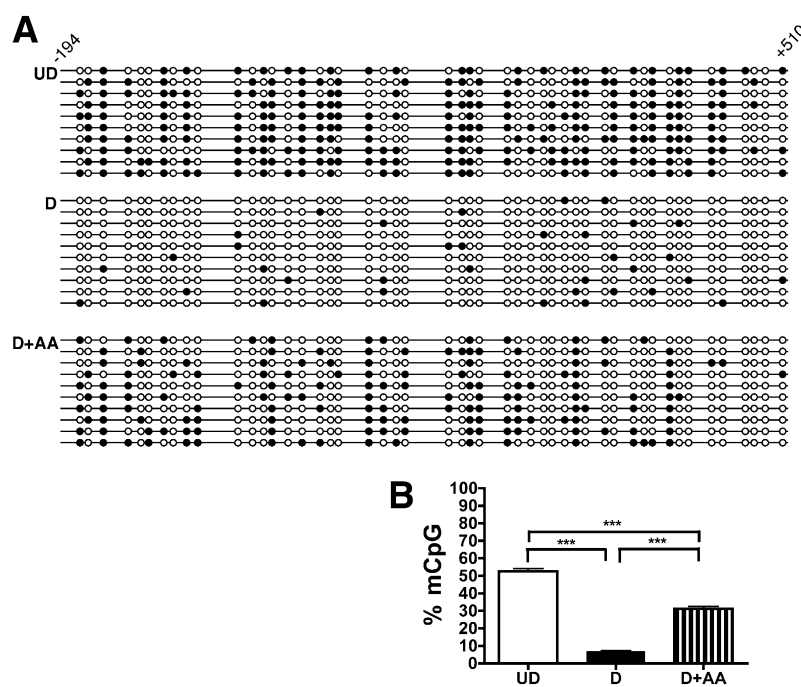


Figure 3—A: Bisulfite sequencing of genomic DNA (-194 to 510, relative to the *Pax3* transcription start site) from UD ESC, or D ESC that had been treated or not with AA (methylated CpGs, ●; unmethylated CpGs, ○). **B:** The mean percentage of methylated CpGs (mCpGs) determined from 10 sequenced clones from each treatment group were analyzed by one-way ANOVA, followed by the Tukey post test. The error bars indicate the standard error. *** $P < 0.001$.

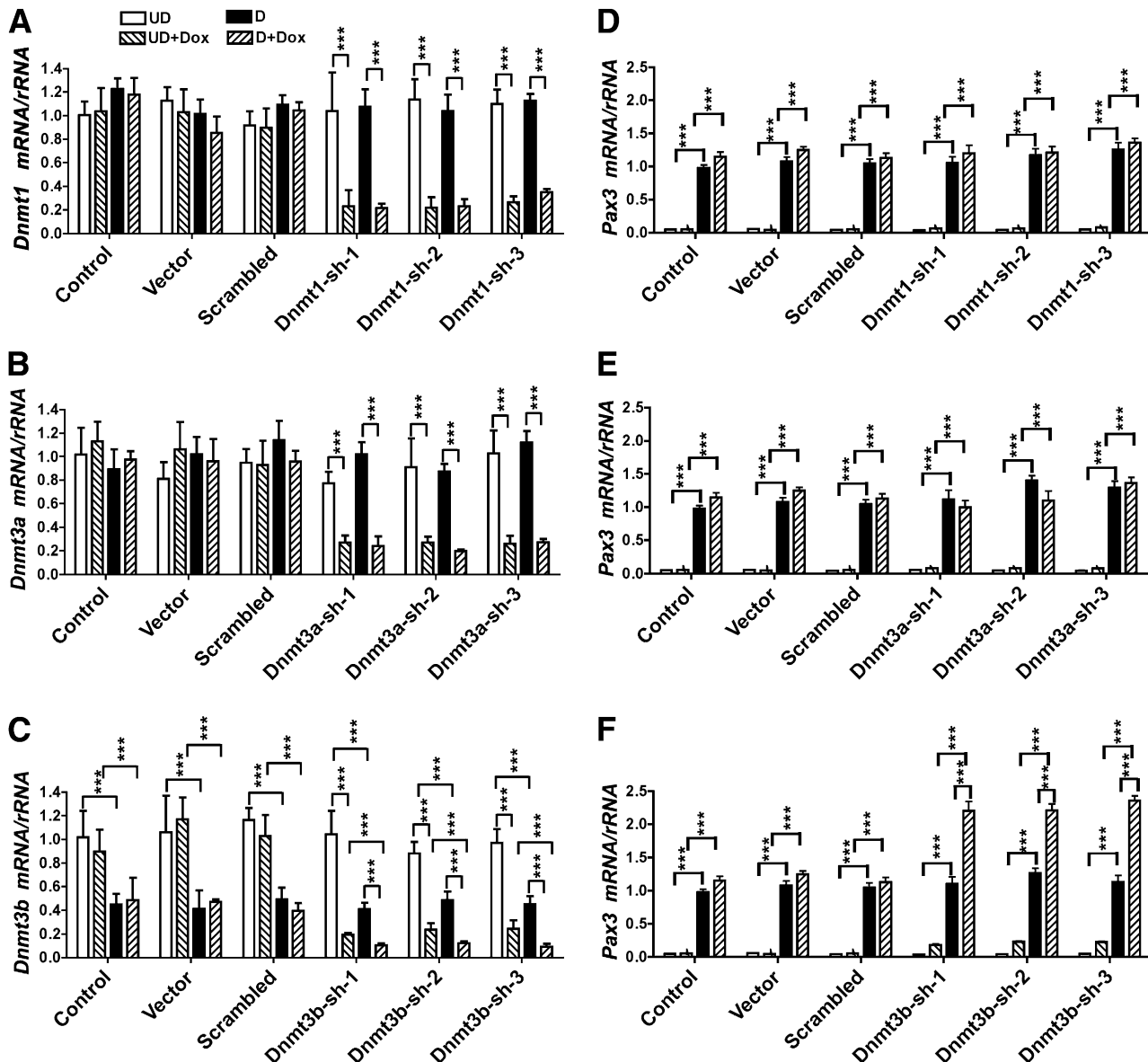


Figure 4—RT-PCR of RNA from ESC stably transfected with Dox-inducible plasmids expressing shRNA targeting *Dnmt1* (A and D), *Dnmt3a* (B and E), or *Dnmt3b* (C and F). Cells were untransfected (control), transfected with empty pSingle plasmid (vector), pSingle containing a scrambled shRNA sequence (scrambled), or pSingle containing one of three different shRNA sequences (-sh-1, -sh-2, -sh-3) targeting each of the DNA methyltransferases. RNA was assayed from UD or D ESC that had been treated or not with Dox. *Dnmt* mRNA was normalized to rRNA and expressed relative to control UD ESC. *Pax3* mRNA was normalized to rRNA and expressed relative to control D ESC. A: *Dnmt1* expression by cells transfected with *Dnmt1* shRNA plasmids or controls. B: *Dnmt3a* expression by cells transfected with *Dnmt3a* shRNA plasmids or controls. C: *Dnmt3b* expression by cells transfected with *Dnmt3b* shRNA plasmids or controls. D: *Pax3* expression by cells transfected with *Dnmt1* shRNA plasmids or controls. E: *Pax3* expression by cells transfected with shRNA plasmids to knock down *Dnmt3a* mRNA or controls. F: *Pax3* expression by cells transfected with shRNA plasmids to knock down *Dnmt3b* mRNA or controls ($n = 4$ replicate culture dishes). Data from each transformed cell line were analyzed individually by one-way ANOVA, followed by the Tukey post test. The error bars indicate the standard error. * $P < 0.001$.**

Fig. 1). Inhibition of *Dnmt* mRNA levels by each of the shRNA sequences was specific for the intended target *Dnmt* transcript and had no effect on either of the other two *Dnmt* transcripts (data not shown). Notably, knocking down *Dnmt1* or *Dnmt3a* had no effect on *Pax3* mRNA in UD or D ESC (Fig. 4D and E). However, there was an increase in *Pax3* mRNA in D ESC and a trend toward increasing *Pax3* mRNA in UD ESC upon knocking down

Dnmt3b mRNA (Fig. 4F). This indicates that *Dnmt3b*, but not *Dnmt1* or *Dnmt3a*, directly or indirectly suppresses *Pax3* expression.

To investigate whether *Dnmt3b* could mediate the inhibition of *Pax3* expression and increased cytosine methylation in response to oxidative stress, the effects of knocking down *Dnmt3b* mRNA on AA-treated differentiating ESC were examined. As shown in Fig. 5A,

hypermethylation of the *Pax3* CpG island in D ESC in response to AA was blocked in cells treated with Dox, but only in cells transfected with the *Dnmt3b* shRNA plasmid. Correspondingly, AA inhibited *Pax3* expression in D ESC that were untransfected, and the inhibition of *Pax3* expression by AA was blocked by treatment with Dox, but only in the cell lines transfected with plasmids containing *Dnmt3b* shRNA (Fig. 5B). As in Fig. 4, Dox treatment increased *Pax3* expression by D cultures not

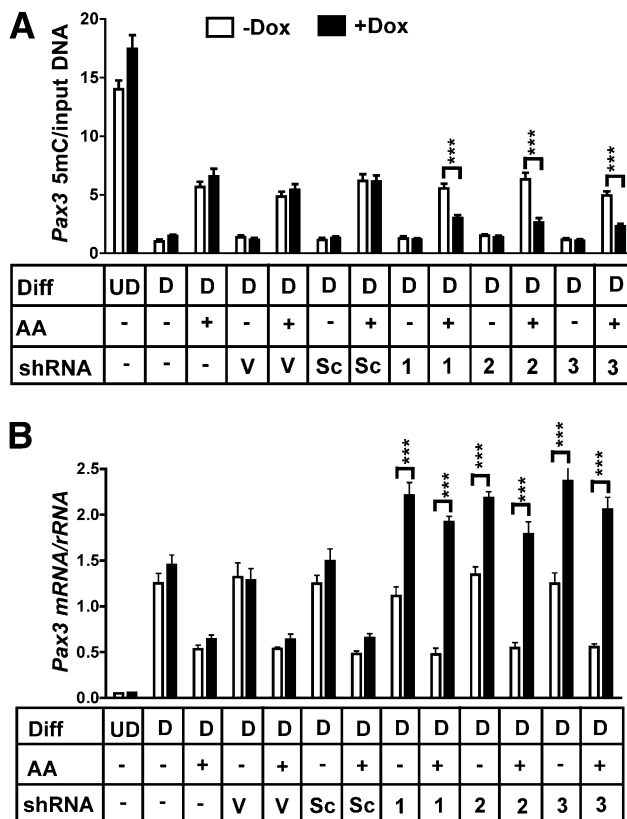


Figure 5—A: RT-PCR of *Pax3* mRNA normalized to *rRNA* from ESC stably transfected with shRNA plasmids targeting only *Dnmt3b* mRNA. Differentiating cultures were treated or not with AA to induce oxidative stress and treated or not with Dox to induce shRNA expression. **B:** mDIP assay of ESC that were cultured alongside the cultures used in A. (Numbers of culture plates used for RT-PCR and mDIP assays are the same as in Fig. 2.) Data from untransfected control cultures (UD, D, D + AA) were analyzed by one-way ANOVA and the Tukey post test. **A:** *Pax3* CpG island methylation was significantly different ($***P < 0.001$) in all treatment groups. **B:** *Pax3* expression was significantly different between UD and D, and between D and D + AA cultures ($***P < 0.001$) but was not different between UD and D + AA cultures ($P > 0.05$). (Significant differences from one-way ANOVA are not indicated in the figure.) Data from shRNA transfected cells were analyzed by two-way ANOVA (treatment group vs. Dox administration), followed by the Bonferroni post test to determine which cultures were affected by Dox treatment. The error bars indicate the standard error. Significant differences between -Dox and +Dox in each treatment group are indicated. AA, AA added (+) or not (-) to differentiating neuronal precursor cultures; Diff, differentiated state (D, differentiating; UD, undifferentiated); shRNA: untransfected (-), empty vector (V), scrambled shRNA (Sc), *Dnmt3b*-sh-1 (1), *Dnmt3b*-sh-2 (2), *Dnmt3b*-sh-3 (3).

treated with AA, but only in cells transfected with plasmids containing *Dnmt3b* shRNA.

Dnmt Activity Regulation by Oxidative Stress

Increased *Dnmt3b*-mediated *Pax3* CpG island methylation stimulated by oxidative stress could be due to increased *Dnmt3b* activity or increased *Dnmt3b* expression, or both. To investigate whether *Dnmt3b* activity could be stimulated by oxidative stress, total *Dnmt* enzyme activity was assayed using nuclear extracts prepared from UD, D, or D ESC treated with AA. As shown in Fig. 6A, total *Dnmt* activity decreased upon ESC differentiation, and the effect of differentiation was inhibited by oxidative stress. However, when we examined mRNA levels of each of the DNA methyltransferases, we found that only expression of *Dnmt3b* decreased upon differentiation and that oxidative stress had no effect on expression of any of the *Dnmt* mRNAs (Fig. 6B). Although the *Dnmt* activity assay could not determine which DNA methyltransferase(s) was responsible for decreased *Dnmt* activity in the nuclear extracts from D ESC, only expression of *Dnmt3b* decreases with differentiation. Therefore, unless there are processes that regulate activity of any of the DNA methyltransferases during differentiation, the decreased abundance of *Dnmt3b* is sufficient to explain the decreased *Dnmt* activity upon differentiation. Moreover, although our results cannot exclude the possibilities that activities of *Dnmt1* and/or *Dnmt3a* are stimulated by oxidative stress, because *Dnmt3b* expression is unaffected by oxidative stress, this indicates that the increased *Dnmt3b*-mediated *Pax3* CpG island methylation during oxidative stress is because *Dnmt3b* enzymatic activity is stimulated by oxidative stress.

DISCUSSION

Pax3 is a gene whose expression in embryonic neuroepithelium and neural crest is essential for neural tube closure and cardiac outflow tract formation (13,14). And yet, its regulation during normal embryonic development is poorly understood. It is expected that induction of *Pax3* expression in temporal- and tissue-specific fashion involves multiple coordinated processes, including induction and assembly of transcription factors and coactivators, modifications of histones by acetylation and methylation, and modification of cytosine methylation within the *Pax3* CpG island or even other regulatory elements such as enhancers. However, which of these processes might be affected by excess glucose metabolism in embryos of diabetic mothers, thereby causing abnormal gene expression and congenital malformations, has not previously been reported. The data reported here indicate that hypermethylation of a *Pax3* CpG island by *Dnmt3b* contributes to *Pax3* silencing before induction of embryonic neuroepithelium and neural crest, and that oxidative stress stimulates *Dnmt3b*-mediated methylation of the *Pax3* CpG island, thereby preserving the methylated state of the same cytosines as in UD embryo cells. This, then, suppresses *Pax3*

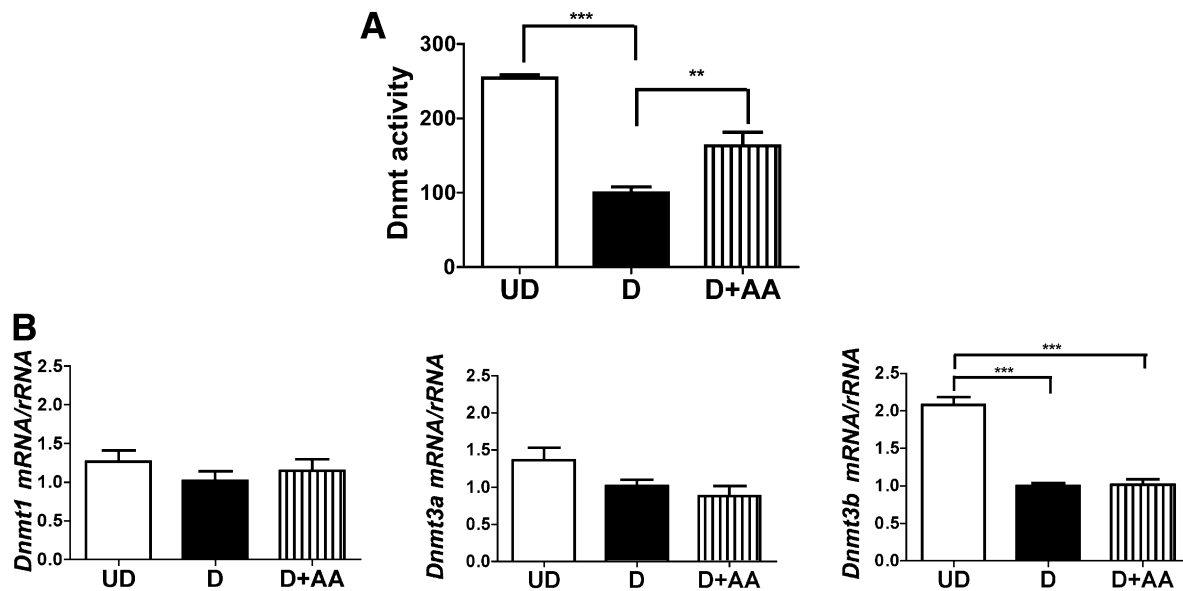


Figure 6—A: Total Dnmt activity using nuclear extracts from UD ESC or D ESC treated or not with AA. Dnmt activity was performed using a colorimetric assay kit as described in RESEARCH DESIGN AND METHODS and expressed as optical density/mg protein per hour ($n = 3$ culture dishes). ** $P < 0.01$; *** $P < 0.001$. **B:** RT-PCR of *Dnmt1*, *Dnmt3a*, or *Dnmt3b*, normalized to rRNA from UD ESC, or D ESC treated or not with AA. The error bars indicate the standard error. *** $P < 0.001$.

expression. A schematic diagram of the regulation of the *Pax3* CpG island during embryonic development and oxidative stress is shown in Fig. 7.

Oxidative stress does not affect all gene expression regulating embryogenesis, because morphology of the neurulating E 8.5 embryo is normal (10), and, as shown here, expression of *Pax7* and *Pax6*, which are also expressed in the neural tube beginning on E 8.5, is unaffected by oxidative stress. Rather, *Pax3* appears to be selectively regulated by oxidative stress resulting from

excess glucose metabolism. Because knocking down *Dnmt3b* mRNA blocks the hypermethylation of the *Pax3* CpG island and the inhibition of *Pax3* expression caused by oxidative stress, this indicates that the CpG island surrounding the *Pax3* transcription start site is an oxidative stress-responsive regulatory element. This is not a characteristic of all CpG islands of embryo-expressed genes, because methylation of the *p53* CpG island and *p53* expression were unaffected by oxidative stress. This said, the responsiveness of the *Pax3* CpG island to

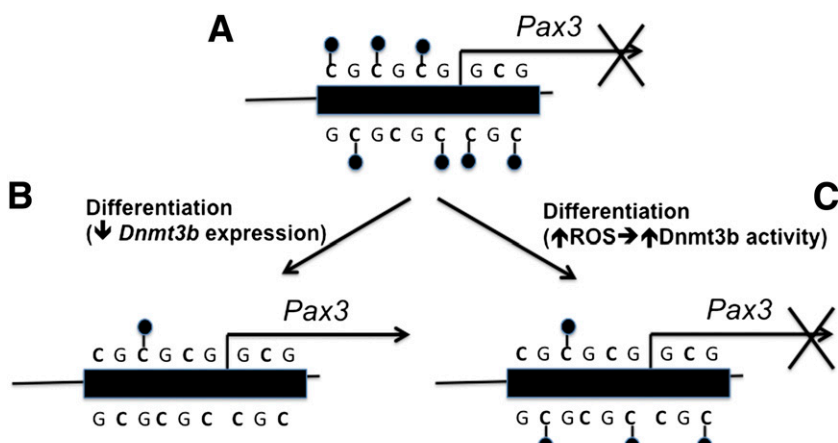


Figure 7—Schematic diagram of regulation of *Pax3* CpG methylation and *Pax3* expression. **A:** In embryonic cells that do not express *Pax3* (blastocysts and UD ESC), the *Pax3* CpG island surrounding the *Pax3* transcription start site is hypermethylated, which contributes to gene silencing. **B:** During normal differentiation (of E 8.5 embryos and ESC induced to form neuronal precursors), decreased *Dnmt3b* expression contributes to decreased *Pax3* CpG island methylation and increased *Pax3* expression. **C:** During differentiation under conditions of oxidative stress, increased reactive oxygen species (ROS) stimulates *Dnmt3b* activity, which preserves *Pax3* CpG island methylation and suppresses *Pax3* expression.

oxidative stress seems to be limited to neuroepithelium and neural crest, because *Pax3* expression by somites is not inhibited by maternal diabetes (10,11), and hypermethylation of the *Pax3* CpG islands after hyperglycemia or oxidative stress was not observed in whole E 8.5 embryos, which contained a greater abundance of somitic progenitors than neuroepithelium and neural crest. The 1.6-kb element that is sufficient for *Pax3* expression in neuroepithelium and neural crest is not sufficient for *Pax3* expression in somites (39). Therefore, differential transcriptional regulation of *Pax3* in somites compared with neuroepithelium and neural crest is a likely explanation for the lack of effect of hyperglycemia and oxidative stress on *Pax3* expression in somites. Further investigation will be needed to understand the tissue-specific regulation of the *Pax3* CpG island by oxidative stress.

The mechanism by which the *Pax3* CpG island becomes hypomethylated during differentiation is not known. The CpG island could be passively demethylated due to decreased methylation of daughter strands during DNA synthesis. This could be caused by decreased expression of *Dnmt3b*, decreased activity of *Dnmt3b*, or other processes, such as histone modifications (24), that divert *Dnmt3b* from the *Pax3* CpG island. Alternatively, the CpG island could be actively demethylated, initiated by oxidation of 5-methylcytosine to 5-hydroxymethylcytosine by the ten-eleven translocation family of enzymes (42). The latter process could occur independent of DNA synthesis. Because embryo cells and ESC are rapidly proliferating when they begin to adopt a neuroepithelial cell fate, passive demethylation would seem the most likely mechanism. This is consistent with the decreased expression of *Dnmt3b* in differentiating ESC. If this is the case, stimulation of *Dnmt3b* activity by oxidative stress might increase *Pax3* CpG island methylation of daughter strands. However, if demethylation is active, *Dnmt3b* might compete with a ten-eleven translocation enzyme for binding to the *Pax3* CpG island. Additional research is necessary to understand how the *Pax3* CpG island becomes demethylated during differentiation and how oxidative stress antagonizes this process.

We previously showed that *Pax3* negatively regulates the p53 tumor suppressor protein by stimulating its degradation in neuronal precursors (35). This appears to be the sole *Pax3* function that is required for neural tube and neural crest development (43,44). We have speculated that *Pax3* is regulated by the transition from predominantly glycolytic to increasingly aerobic metabolism that occurs as stem cells start to differentiate so that it can titrate the abundance of p53, which promotes aerobic metabolism and terminal differentiation (9). Thus, oxidative stress resulting from excess glucose metabolism may disturb the metabolic cues that lead to *Pax3* gene activation.

We have also shown that increased embryo glucose metabolism, resulting from maternal hyperglycemia, causes embryo hypoxia, that embryo hypoxia induces oxidative

stress, that oxidative stress stimulates activity of the enzyme AMPK, and that resulting AMPK activity inhibits *Pax3* expression (22,31). Activation of enzymes, such as AMPK, which can translocate to the nucleus (45) and activate transcription factors and coactivators (46–48), can explain how fuel metabolism can regulate *Pax3* expression. However, whether regulation of *Pax3* by AMPK might be mediated by increased *Dnmt3b* activity still remains to be determined.

Others have shown that transient hyperglycemia causes persistent changes in histone methylation patterns that can explain “metabolic memory” despite normoglycemia (49,50). It is intriguing to speculate that stimulation of *Dnmt3b* activity by transient hyperglycemia could also have long-lasting effects on cytosine methylation of cells involved in diabetes complications in general.

Acknowledgments. The authors thank Dr. Jin Hyuk Jung of the Loeken Laboratory at the Joslin Diabetes Center for assistance with assay of embryo and ESC *Pax* gene expression.

Funding. M.R.L. was supported by a grant from the National Institute of Diabetes and Digestive and Kidney Diseases under award number R01DK058300 and was assisted by core facilities supported by a Diabetes Endocrine Research Center grant, P01DK036836, to the Joslin Diabetes Center and by the DNA Resource Core provided by the Dana-Farber/Harvard Cancer Center.

Duality of Interest. No potential conflicts of interest relevant to this article were reported.

Author Contributions. D.W. designed and performed the experiments. M.R.L. designed the experiments and wrote the manuscript. M.R.L. is the guarantor of this work and, as such, had full access to all the data in the study and takes responsibility for the integrity of the data and the accuracy of the data analysis.

Prior Presentation. Portions of this study were presented at the 72nd Scientific Sessions of the American Diabetes Association, Philadelphia, PA, 8–12 June 2012.

References

1. Evers IM, de Valk HW, Visser GH. Risk of complications of pregnancy in women with type 1 diabetes: nationwide prospective study in the Netherlands. *BMJ* 2004;328:915–919
2. Loffredo CA, Wilson PD, Ferencz C. Maternal diabetes: an independent risk factor for major cardiovascular malformations with increased mortality of affected infants. *Teratology* 2001;64:98–106
3. Schaefer-Graf UM, Buchanan TA, Xiang A, Songster G, Montoro M, Kjos SL. Patterns of congenital anomalies and relationship to initial maternal fasting glucose levels in pregnancies complicated by type 2 and gestational diabetes. *Am J Obstet Gynecol* 2000;182:313–320
4. Towner D, Kjos SL, Leung B, et al. Congenital malformations in pregnancies complicated by NIDDM. *Diabetes Care* 1995;18:1446–1451
5. Wren C, Birrell G, Hawthorne G. Cardiovascular malformations in infants of diabetic mothers. *Heart* 2003;89:1217–1220
6. Correa A, Gilboa SM, Besser LM, et al. Diabetes mellitus and birth defects. *Am J Obstet Gynecol* 2008;199:e237.e9
7. Becerra JE, Khouri MJ, Cordero JF, Erickson JD. Diabetes mellitus during pregnancy and the risks for specific birth defects: a population-based case-control study. *Pediatrics* 1990;85:1–9
8. Mills JL, Baker L, Goldman AS. Malformations in infants of diabetic mothers occur before the seventh gestational week. Implications for treatment. *Diabetes* 1979;28:292–293

9. Zabihi S, Loeken MR. Understanding diabetic teratogenesis: where are we now and where are we going? *Birth Defects Res A Clin Mol Teratol* 2010;88:779–790
10. Phelan SA, Ito M, Loeken MR. Neural tube defects in embryos of diabetic mice: role of the Pax-3 gene and apoptosis. *Diabetes* 1997;46:1189–1197
11. Morgan SC, Relaix F, Sandell LL, Loeken MR. Oxidative stress during diabetic pregnancy disrupts cardiac neural crest migration and causes outflow tract defects. *Birth Defects Res A Clin Mol Teratol* 2008;82:453–463
12. Fine EL, Horal M, Chang TI, Fortin G, Loeken MR. Evidence that elevated glucose causes altered gene expression, apoptosis, and neural tube defects in a mouse model of diabetic pregnancy. *Diabetes* 1999;48:2454–2462
13. Auerbach R. Analysis of the developmental effects of a lethal mutation in the house mouse. *J Exp Zool* 1954;127:305–329
14. Franz T. Persistent truncus arteriosus in the Splotch mutant mouse. *Anat Embryol (Berl)* 1989;180:457–464
15. Simán CM, Eriksson UJ. Vitamin E decreases the occurrence of malformations in the offspring of diabetic rats. *Diabetes* 1997;46:1054–1061
16. Simán CM, Eriksson UJ. Vitamin C supplementation of the maternal diet reduces the rate of malformation in the offspring of diabetic rats. *Diabetologia* 1997;40:1416–1424
17. Sivan E, Reece EA, Wu YK, Homko CJ, Polansky M, Borenstein M. Dietary vitamin E prophylaxis and diabetic embryopathy: morphologic and biochemical analysis. *Am J Obstet Gynecol* 1996;175:793–799
18. Viana M, Herrera E, Bonet B. Teratogenic effects of diabetes mellitus in the rat. Prevention by vitamin E. *Diabetologia* 1996;39:1041–1046
19. Trocino RA, Akazawa S, Ishibashi M, et al. Significance of glutathione depletion and oxidative stress in early embryogenesis in glucose-induced rat embryo culture. *Diabetes* 1995;44:992–998
20. Sakamaki H, Akazawa S, Ishibashi M, et al. Significance of glutathione-dependent antioxidant system in diabetes-induced embryonic malformations. *Diabetes* 1999;48:1138–1144
21. Chang TI, Horal M, Jain SK, Wang F, Patel R, Loeken MR. Oxidant regulation of gene expression and neural tube development: insights gained from diabetic pregnancy on molecular causes of neural tube defects. *Diabetologia* 2003;46:538–545
22. Li R, Chase M, Jung SK, Smith PJS, Loeken MR. Hypoxic stress in diabetic pregnancy contributes to impaired embryo gene expression and defective development by inducing oxidative stress. *Am J Physiol Endocrinol Metab* 2005;289:E591–E599
23. Smith ZD, Chan MM, Mikkelsen TS, et al. A unique regulatory phase of DNA methylation in the early mammalian embryo. *Nature* 2012;484:339–344
24. Meissner A, Mikkelsen TS, Gu H, et al. Genome-scale DNA methylation maps of pluripotent and differentiated cells. *Nature* 2008;454:766–770
25. Borgel J, Guibert S, Li Y, et al. Targets and dynamics of promoter DNA methylation during early mouse development. *Nat Genet* 2010;42:1093–1100
26. Smith ZD, Meissner A. DNA methylation: roles in mammalian development. *Nat Rev Genet* 2013;14:204–220
27. Fouse SD, Shen Y, Pellegrini M, et al. Promoter CpG methylation contributes to ES cell gene regulation in parallel with Oct4/Nanog, P_cG complex, and histone H3 K4/K27 trimethylation. *Cell Stem Cell* 2008;2:160–169
28. Mikkelsen TS, Ku M, Jaffe DB, et al. Genome-wide maps of chromatin state in pluripotent and lineage-committed cells. *Nature* 2007;448:553–560
29. Illingworth R, Kerr A, Desousa D, et al. A novel CpG island set identifies tissue-specific methylation at developmental gene loci. *PLoS Biol* 2008;6:e22
30. Reik W, Dean W, Walter J. Epigenetic reprogramming in mammalian development. *Science* 2001;293:1089–1093
31. Wu Y, Viana M, Thirumangalathu S, Loeken MR. AMP-activated protein kinase mediates effects of oxidative stress on embryo gene expression in a mouse model of diabetic embryopathy. *Diabetologia* 2012;55:245–254
32. Jung JH, Wang XD, Loeken MR. Mouse embryonic stem cells established in physiological-glucose media express the high KM Glut2 glucose transporter expressed by normal embryos. *Stem Cells Transl Med* 2013;2:929–934
33. Weber M, Davies JJ, Wittig D, et al. Chromosome-wide and promoter-specific analyses identify sites of differential DNA methylation in normal and transformed human cells. *Nat Genet* 2005;37:853–862
34. Kumaki Y, Oda M, Okano M. QUMA: Quantification Tool for Methylation Analysis. *Nucleic Acids Res* 2008;36:W170–W175
35. Wang XD, Morgan SC, Loeken MR. Pax3 stimulates p53 ubiquitination and degradation independent of transcription. *PLoS ONE* 2011;6:e29379
36. Chalepakis G, Tremblay P, Gruss P. Pax genes, mutants and molecular function. *J Cell Sci Suppl* 1992;16:61–67
37. Goulding MD, Lumsden A, Gruss P. Signals from the notochord and floor plate regulate the region-specific expression of two Pax genes in the developing spinal cord. *Development* 1993;117:1001–1016
38. Appella E, Anderson CW. Post-translational modifications and activation of p53 by genotoxic stresses. *Eur J Biochem* 2001;268:2764–2772
39. Natoli TA, Ellsworth MK, Wu C, Gross KW, Pruitt SC. Positive and negative DNA sequence elements are required to establish the pattern of *Pax3* expression. *Development* 1997;124:617–626
40. Goulding MD, Chalepakis G, Deutsch U, Erselius JR, Gruss P. Pax-3, a novel murine DNA binding protein expressed during early neurogenesis. *EMBO J* 1991;10:1135–1147
41. Clark SJ, Statham A, Stirzaker C, Molloy PL, Frommer M. DNA methylation: bisulphite modification and analysis. *Nat Protoc* 2006;1:2353–2364
42. Branco MR, Ficz G, Reik W. Uncovering the role of 5-hydroxymethylcytosine in the epigenome. *Nat Rev Genet* 2012;13:7–13
43. Pani L, Horal M, Loeken MR. Rescue of neural tube defects in Pax-3-deficient embryos by p53 loss of function: implications for Pax-3-dependent development and tumorigenesis. *Genes Dev* 2002;16:676–680
44. Morgan SC, Lee H-Y, Relaix F, Sandell LL, Levorse JM, Loeken MR. Cardiac outflow tract septation failure in Pax3-deficient embryos is due to p53-dependent regulation of migrating cardiac neural crest. *Mech Dev* 2008;125:757–767
45. McGee SL, Howlett KF, Starkie RL, Cameron-Smith D, Kemp BE, Hargreaves M. Exercise increases nuclear AMPK alpha2 in human skeletal muscle. *Diabetes* 2003;52:926–928
46. Yang W, Hong YH, Shen XQ, Frankowski C, Camp HS, Leff T. Regulation of transcription by AMP-activated protein kinase: phosphorylation of p300 blocks its interaction with nuclear receptors. *J Biol Chem* 2001;276:38341–38344
47. Hong YH, Varanasi US, Yang W, Leff T. AMP-activated protein kinase regulates HNF4alpha transcriptional activity by inhibiting dimer formation and decreasing protein stability. *J Biol Chem* 2003;278:27495–27501
48. Solaz-Fuster MC, Gimeno-Alcañiz JV, Casado M, Sanz P. TRIP6 transcriptional co-activator is a novel substrate of AMP-activated protein kinase. *Cell Signal* 2006;18:1702–1712
49. Brasacchio D, Okabe J, Tikellis C, et al. Hyperglycemia induces a dynamic cooperativity of histone methylase and demethylase enzymes associated with gene-activating epigenetic marks that coexist on the lysine tail. *Diabetes* 2009;58:1229–1236
50. El-Osta A, Brasacchio D, Yao D, et al. Transient high glucose causes persistent epigenetic changes and altered gene expression during subsequent normoglycemia. *J Exp Med* 2008;205:2409–2417